ISSN: 1999-6691, e-ISSN: 2782-3709 DOI: 10.7242/1999-6691/2026.19.1.4

Research article

Analysis of the bifurcation structure near the excitation threshold of convection during uniform fluid infiltration through a slightly asymmetric porous chip

D.A. Bratsun

Perm National Research Polytechnic University, Perm, Russian Federation

Fluid-saturated porous scaffolds are crucial components of flow perfusion bioreactors, which act as microfluidic chips. These devices are used to grow cell cultures in a constant, steady-state environment through maintaining a continuous flow of nutrient-rich solution. Cell proliferation often occurs in non-isothermal conditions, which under gravity can lead to the onset of thermal convection. In this paper, we consider the problem of convection excitation in a porous chip heated from below, across which uniform pumping of an incompressible fluid is carried out. It has been known that incorporating a fluid-saturated porous structure into highly conductive impermeable medium leads to the fact that the boundary value problem takes on the cosymmetry property for any simply connected 2-D shape of the domain. This causes branching of one-parameter families of heterogeneous equilibrium states. Note however that even weak fluid pumping across the porous medium leads to cosymmetry breaking and the type of dynamic behavior of the system in this case depends on the domain symmetry. If under reflection the pumping domain is symmetric about the vertical axis, the resulting convection will be stationary. In the asymmetric domain, periodic oscillations are excited. In this paper, we investigate the bifurcation structure near the convection excitation threshold occurring in a weakly asymmetric domain. The main focus is on the transition from stationary to oscillatory convection. The study of the system includes the following issues: finding the basic state of the system analytically; linear analysis of its stability using the Galerkin method; analysis of weakly nonlinear solutions near the first bifurcation point using the method of multiple time scales. It has been shown that branching of solutions near the excitation threshold of convection in a weakly non-cosymmetric system of equations defined in a weakly asymmetric domain is of surprisingly complex nature. The transition process includes the Andronov–Hopf bifurcation, the birth and death of limiting cycles at the backward and forward tangential bifurcations of a pair of equilibria, respectively; and the formation of homoclinic trajectories. Stability maps are constructed on the planes of control parameters of the problem: the Rayleigh number for the porous medium, the thermal Péclet number, and the chip tilt angle, which acts as a symmetry imperfection parameter. Bifurcation diagrams of a dynamic system on its slow manifold are presented.

Keywords: porous medium, convective instability, bifurcation, symmetry, cosymmetry

Received: 13.10.2025 / *Published online*: 01.06.2026

1. Introduction

Filtration convection of an incompressible fluid saturating a porous medium invariably attracts the attention of researchers because of the widespread occurrence of this phenomenon in nature and technology [1]. Traditional fields of application include filtration through heterogeneous media in oil and gas production [2], the arrangement of municipal and industrial waste disposal sites [3, 4], reaction–diffusion–convection processes in the chemical industry [5], and others. Among relatively new areas, one may mention tissue engineering, which uses synthetic porous materials for growing cell cultures [6–9]. The solid matrix here serves either as a framework (scaffold) for the tissue being formed or as a bone implant (in regenerative medicine). Cell division in a bioreactor requires a continuous supply of nutrients. It is also worth mentioning the problem of the collective behavior of emperor penguins or robots. As it turns out, this problem can also be formulated on the basis of the concept of thermal convection in a porous medium [10].

If one considers the problem of convective stability of a fluid saturating a homogeneous porous layer heated from below, then initially it was apparently regarded as close to the classical Rayleigh–Bénard problem [11, 12]. As in a homogeneous fluid, at a certain value of the Rayleigh number the mechanical equilibrium becomes unstable, and steady convection arises as a result of a pitchfork bifurcation. The equation of motion of a fluid in a porous medium is written in a much simpler form than in the case of a homogeneous fluid flow; therefore, some researchers considered filtration problems an excellent test bed for refining the tools of nonlinear dynamics and bifurcation theory [13]. A turning point was the work of D.V. Lyubimov [14], in which, by solving the problem of the onset of thermal convection in a horizontal

©Authors 2026 Translation of the original article in Russian This is an open access article under the CC BY 4.0 license

porous cylinder with perfectly thermally conducting boundaries, it was shown that mechanical equilibrium is replaced not by one or two equilibrium states, but by an entire one-parameter family. Moreover, this conclusion proved valid for an arbitrary simply connected shape of the cylinder cross section. The result appeared unusual, since the problem possessed no visible symmetries with a free parameter; nevertheless, the theoretical prediction was confirmed experimentally [15].

A careful examination in [14] of what seemed to be a standard problem formulation led to the need to apply the theory of cosymmetry proposed by V.I. Yudovich [16]. Cosymmetry is understood as the property of a problem to possess a hidden conserved integral whose origin is not associated with symmetry; in dynamical systems with cosymmetry, all equilibrium states are classified either as cosymmetric or as non-cosymmetric. The latter are always families. Subsequently, the theory of cosymmetry was developed in a series of works by V.I. Yudovich and his students [17–22]. The bifurcations of isolated cosymmetric equilibria [17], the branching of one-parameter families of non-cosymmetric equilibria [17, 20–22], and bifurcations under cosymmetry breaking [19] were investigated. The latter issue was also considered in [23], where the authors discovered an interesting fact: in the case of vertical fluid pumping, the cosymmetry of the problem is broken and the degeneracy is lifted; the scenario of the breakup of a one-parameter family near the first bifurcation point is governed by the symmetry of the domain. If the cross section of the horizontal porous cylinder is symmetric with respect to horizontal reflection, steady convection is observed. If this condition is not satisfied, then a limit cycle exists near the threshold. However, the manner in which the transition from periodic convection to steady convection and back occurs has not been investigated. The present work is intended to fill this gap. In practical applications, an increasing number of problems are encountered in which uniform seepage of an incompressible fluid through a porous medium is of significant importance. The ability to switch convective regimes in porous chips by means of a weak external action appears useful in various devices. In addition, vertical pumping has not received sufficient attention in the literature, although it is less energy-intensive. This approach can be implemented, for example, by placing a reservoir with fluid directly above the convective system and allowing the fluid to seep through the porous medium by gravity.

This article may also be viewed as an analytical study of bifurcation analysis. All processes are considered in the vicinity of the first bifurcation point. Therefore, the asymptotic theory can be constructed from the formulation of the problem through to obtaining the normal form for the branching of solutions on the slow manifold of the system under study and estimating its bifurcation structure. Although direct numerical simulation of hydrodynamic systems has become predominant in recent years, physicists should not lose their historical expertise in perturbation theory, which dates back to the works of Newton.

2. Mathematical formulation of the problem

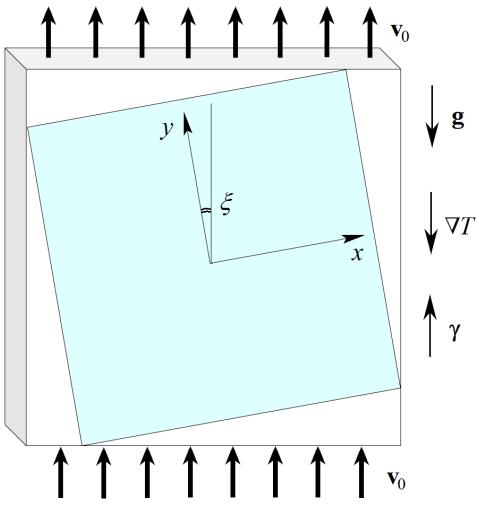


Fig. 1. Schematic representation of a system with a chip (shaded) – a weakly asymmetric region of a porous medium embedded in a massif, through which uniform seepage of an incompressible fluid occurs; the system is heated from below

Consider the motion of an incompressible fluid with dynamic viscosity η and density ρ_0, filling an infinitely extended horizontal porous cylinder with solid permeable boundaries, which is surrounded on all sides by a solid massif with high thermal conductivity. Let the cross section of the cylinder be a square with characteristic size h, capable of having different inclinations relative to the direction of gravitational acceleration $\mathbf{g} = -g\boldsymbol{\gamma}$, where $\boldsymbol{\gamma}$ — is a unit vector defining the inclination angle ξ of the rectangular coordinate system $\{x,y\}$ (Fig. 1):

$$\boldsymbol{\gamma}: (\sin(\xi),\cos(\xi)). \tag{1}$$

The massif with the cylinder is heated from below in such a way that, in any situation, a mechanical equilibrium of the fluid characterized by the equilibrium temperature gradient $-A\boldsymbol{\gamma}$ can exist. Although the cylinder considered is mathematically infinite, in practice a good approximation to this theoretical construction is a cylinder of finite length whose side walls are insulated from heat fluxes along the cylinder. In [24, 25] it was shown that if the cylinder is shorter along its axis than the characteristic size h, then

two-dimensional disturbances are the most dangerous. This justifies the sufficiency of studying only the class of two-dimensional convective motions, which substantially simplifies the analysis. Therefore, in Fig. 1 the porous cylinder is shown as a square prism flattened along the axis of rotation perpendicular to the plane of the figure.

Taking the above into account, the governing equations of filtration convection in the Darcy–Boussinesq approximation take the following form [13]:

$$\nabla\cdot\mathbf{v}=0, \tag{2}$$

$$-\frac{1}{\rho_0}\nabla P'+g\beta_0 T\boldsymbol{\gamma}-\frac{\nu}{K}\mathbf{v}=0, \tag{3}$$

$$b\frac{\partial T}{\partial t}+\mathbf{v}\cdot\nabla T=\chi\Delta\,\mathrm{T}, \tag{4}$$

where $\mathbf{v}$ — is the filtration velocity of the fluid, T — is the temperature, P' — is the pressure, β_0 — is the coefficient of thermal volumetric expansion, ν — is the kinematic viscosity coefficient, K — is the permeability coefficient of the medium, b — is the ratio of the heat capacities of the medium and the fluid, and χ — is the effective thermal diffusivity of the porous matrix saturated with fluid.

Let us discuss the boundary conditions for the fields in (2)–(4). Assume that uniform fluid injection with velocity $\mathbf{v}_0=v_0\boldsymbol{\gamma}$ occurs through the lower boundary of the cylinder, while uniform withdrawal with the same velocity occurs through the upper boundary (Fig. 1). Then, on the boundary G, the following condition is obtained for the normal component of velocity:

$$v_n|_G=v_0\,\mathbf{n}\cdot\boldsymbol{\gamma}, \tag{5}$$

where $\mathbf{n}$ — is the unit normal vector to G. Since the equation of motion (3) is linear, condition (5) is quite sufficient to determine the velocity field.

Because the chip is surrounded on all sides by a solid massif with high thermal conductivity, an equilibrium temperature distribution depending on its shape is established at its boundaries, while all disturbances are efficiently removed from the boundary into the massif and decay:

$$T|_G=T_0. \tag{6}$$

Thus, the boundary-value problem (2)–(6) determines the dynamics of convective motions in the chip. On the one hand, boundary condition (6) guarantees that, in the absence of fluid pumping, this problem has cosymmetry [14, 16]. A low pumping intensity makes problem (2)–(6) weakly non-cosymmetric. On the other hand, rotation of the cylinder (chip) about its axis makes it possible to consider both symmetric and asymmetric domains. Small angles ξ make problem (2)–(6) weakly asymmetric. By combining the parameter values, one can obtain and discuss various situations.

We represent the general solution of problem (2)–(6) as the sum of the basic state and its finite disturbances:

$$\begin{pmatrix}\mathbf{v}(t,x,y)\\ T(t,x,y)\\ P'(t,x,y)\end{pmatrix}=\begin{pmatrix}\mathbf{v}_0\\ T_0(x,y)\\ p_0\end{pmatrix}+\begin{pmatrix}\mathbf{u}(t,x,y)\\ \theta(t,x,y)\\ p(t,x,y)\end{pmatrix}. \tag{7}$$

By analogy with [14, 23], we nondimensionalize the physical quantities using the following scales: h — length, χ/h — velocity, bh^2/χ — time, $\nu\chi\rho_0/K$ — pressure, and $(\nu\chi A/g\beta K)^{1/2}$ — temperature. This procedure makes it possible to symmetrize the linear operator with respect to velocity and temperature disturbances. Substituting (7) into (2)–(6) and resolving the equations for the basic state, taking into account (1), we arrive at the dimensionless form of the solution for the uniform undisturbed flow through the chip:

$$\mathbf{v}_0:(v_0\sin(\xi),v_0\cos(\xi)), \tag{8}$$

$$\nabla T_0:\left(\frac{\mathrm{PeRa}}{2\mathrm{sh}(\mathrm{Pe}/2)}e^{\mathrm{Pe}\sin(\xi)x}\sin(\xi),\frac{\mathrm{PeRa}}{2\mathrm{sh}(\mathrm{Pe}/2)}e^{\mathrm{Pe}\cos(\xi)y}\cos(\xi)\right). \tag{9}$$

In expressions (8), (9), two dimensionless parameters appear that determine the evolution of convective flows — the Rayleigh number for a porous medium and the thermal Péclet number:

$$\mathrm{Ra}=h\sqrt{\frac{g\beta KA}{\nu\chi}},\quad \mathrm{Pe}=\frac{v_0h}{\chi}. \tag{10}$$

Using the incompressibility condition (2), we introduce the stream function:

$$u_x = \frac{\partial \psi}{\partial y}, \quad u_y = -\frac{\partial \psi}{\partial x},$$

and rewrite the problem in terms of the stream function and temperature:

$$\Delta\psi - \mathrm{Ra}\left(\cos(\xi)\frac{\partial\theta}{\partial x} - \sin(\xi)\frac{\partial\theta}{\partial y}\right) = 0, \tag{11}$$

$$\frac{\partial\theta}{\partial t} + J(\psi,\theta) =$$

$$= \Delta\theta + \frac{\mathrm{PeRa}}{2\mathrm{sh}(\mathrm{Pe}/2)}\left(e^{\mathrm{Pe}\cos(\xi)y}\cos(\xi)\frac{\partial\psi}{\partial x} - e^{\mathrm{Pe}\sin(\xi)x}\sin(\xi)\frac{\partial\psi}{\partial y}\right) - \mathrm{Pe}\left(\sin(\xi)\frac{\partial\theta}{\partial x} + \cos(\xi)\frac{\partial\theta}{\partial y}\right), \tag{12}$$

$$\psi|_G = 0, \quad \theta|_G = 0, \tag{13}$$

where, for brevity, the Jacobian is denoted by:

$$J(\psi,\theta) \equiv \frac{\partial\psi}{\partial x}\frac{\partial\theta}{\partial y} - \frac{\partial\psi}{\partial y}\frac{\partial\theta}{\partial x}.$$

Let us present important limiting cases for the system (11)–(13). Thus, when fluid pumping through the porous chip ceases ($\mathrm{Pe} \to 0$), we have:

$$\Delta\psi - \mathrm{Ra}\left(\cos(\xi)\frac{\partial\theta}{\partial x} - \sin(\xi)\frac{\partial\theta}{\partial y}\right) = 0,$$

$$\frac{\partial\theta}{\partial t} + J(\psi,\theta) = \Delta\theta + \mathrm{Ra}\left(\cos(\xi)\frac{\partial\psi}{\partial x} - \sin(\xi)\frac{\partial\psi}{\partial y}\right), \tag{14}$$

$$\psi|_G = 0, \quad \theta|_G = 0.$$

If the problem is invariant under horizontal reflection ($\xi \to 0$), we obtain:

$$\Delta\psi - \mathrm{Ra}\frac{\partial\theta}{\partial x} = 0,$$

$$\frac{\partial\theta}{\partial t} + J(\psi,\theta) = \Delta\theta + \frac{\mathrm{PeRa}}{2\mathrm{sh}(\mathrm{Pe}/2)}e^{\mathrm{Pe}y}\frac{\partial\psi}{\partial x} - \mathrm{Pe}\frac{\partial\theta}{\partial y}, \tag{15}$$

$$\psi|_G = 0, \quad \theta|_G = 0.$$

Finally, if both limiting cases (14) and (15) are valid, we have:

$$\Delta\psi - \mathrm{Ra}\frac{\partial\theta}{\partial x} = 0,$$

$$\frac{\partial\theta}{\partial t} + J(\psi,\theta) = \Delta\theta + \mathrm{Ra}\frac{\partial\psi}{\partial x}, \tag{16}$$

$$\psi|_G = 0, \quad \theta|_G = 0.$$

Let us show that problem (16) possesses the property of cosymmetry [16]. Let the set of functions θ form a Hilbert space. Then, in this space, equations (16) can be represented in operator form:

$$\hat{Q}\theta = \frac{\partial\theta}{\partial t}, \quad \hat{L}\theta = \psi.$$

Here the operator $\hat{Q}$ is evolutionary and nonlinear, functionally dependent on ψ, while the operator $\hat{L}$ is a linear integro-differential operator that is the solution of the two-dimensional Poisson equation.

We introduce the scalar product of two arbitrary functions:

$$\langle a(x,y),b(x,y)\rangle = \int\limits_{-0.5}^{0.5}\int\limits_{-0.5}^{0.5} a(x,y)b(x,y)\,dxdy. \tag{17}$$

Using (17), we arrive at the expression:

$$\left\langle \hat{L}\theta,\hat{Q}\theta \right\rangle = 0. \tag{18}$$

Thus, in (18) the operators form a nontrivial cosymmetric pair.

In [16] it was proved that, in a Hilbert space, the orthogonality of the operators (18) leads to degeneracy of the stationary solutions of problem (16) that do not simultaneously make both operators vanish. Such equilibria are called non-cosymmetric. For example, in problem (16), these are any stationary solutions that describe convective motions of the fluid. The mechanical equilibrium of the fluid, for which the stream function and temperature disturbance are equal to zero, belongs to the class of nondegenerate cosymmetric equilibria. In this case, the Péclet number acts as a parameter that breaks property (18). In problem (11)–(13), it may be called the cosymmetry imperfection parameter. The cuvette inclination angle ξ, conversely, is a parameter of discrete-symmetry imperfection in problem (11)–(13).

3. Linear analysis of the mechanical equilibrium of the fluid

We perform a linear stability analysis of the basic state (8), (9). We first consider the problem without pumping ($\mathrm{Pe}=0$), which admits an analytical solution. Let us turn to normal disturbances of the form:

$$\begin{pmatrix} \psi(t,x,y) \\ \theta(t,x,y) \end{pmatrix} = \begin{pmatrix} \hat{\psi}(x,y) \\ \hat{\theta}(x,y) \end{pmatrix} e^{\lambda t},$$

where λ — is the disturbance increment, and $\hat{\psi}$ and $\hat{\theta}$ — are disturbance amplitudes depending only on the coordinates.

Linearizing problem (14) near the threshold of convection onset, we obtain the following problem for small monotonic disturbances ($\lambda=0$):

$$\begin{gathered} \Delta\psi - \mathrm{Ra}\left(\cos(\xi)\frac{\partial\theta}{\partial x} - \sin(\xi)\frac{\partial\theta}{\partial y}\right) = 0, \\ \Delta\theta + \mathrm{Ra}\left(\cos(\xi)\frac{\partial\psi}{\partial x} - \sin(\xi)\frac{\partial\psi}{\partial y}\right) = 0, \\ \psi|_G = 0, \quad \theta|_G = 0. \end{gathered} \tag{19}$$

Here and below, the hats over the amplitude notations are omitted for simplicity.

As can be seen, problem (19) is invariant with respect to the substitution

$$\psi \to \theta, \quad \theta \to -\psi.$$

Thus, if the functions ψ and θ satisfy equations (19), then the pair of functions θ and $-\psi$ will also be a solution. It is important to note that these solutions are linearly independent; therefore, each eigenvalue of (19) is doubly degenerate. This is a direct consequence of the presence of the cosymmetry property (18) in problem (14). Introducing the complex function

$$\Phi = \psi + i\,\theta,$$

we obtain, instead of (19), a problem of the form:

$$\Delta\Phi + i\mathrm{Ra}\left(\cos(\xi)\frac{\partial\Phi}{\partial x} - \sin(\xi)\frac{\partial\Phi}{\partial y}\right) = 0, \quad \Phi|_G = 0. \tag{20}$$

We apply the following transformation to (20):

$$\Phi(x,y) = \Omega(x,y)e^{(-i\mathrm{Ra}/2)(x\cos(\xi)-y\sin(\xi))}. \tag{21}$$

As a result, we have:

$$\Delta\Omega+\frac{\mathrm{Ra}^2}{4}\Omega=0,\quad \Omega|_G=0. \tag{22}$$

Boundary-value problem (22) describes the natural vibrations of a plate with clamped edges. For a square domain, it is readily solved analytically. As a result, we obtain an expression for the neutral stability curve of the basic state (8), (9):

$$\mathrm{Ra}_0(\xi)=\frac{2\pi}{\cos(\pi/4-\xi)}. \tag{23}$$

The value (23) corresponds to the eigenfunctions of problem (19), which, taking into account (21) and (22), can be written as

$$\psi(x,y)=\cos(\sqrt{2}\pi\,(x\cos(\xi)-y\sin(\xi)))\cos(\pi x)\cos(\pi y), \tag{24}$$

$$\theta(x,y)=-\sin(\sqrt{2}\,\pi\,(x\cos(\xi)-y\sin(\xi)))\cos(\pi x)\cos(\pi y). \tag{25}$$

Figure 2*a* shows the stability map of the basic state in the plane of the parameters Ra and ξ. The neutral curve for the problem without pumping ($\mathrm{Pe}=0$) (23) is shown by a thick solid line. The substantial decrease in the stability threshold upon rotation of the chip about its axis is associated with the fact that, for a fixed temperature gradient, its vertical dimension increases with increasing ξ. The angle $\xi=\pi/4$ corresponds to a rhombic shape of the chip cross section, which provides its maximum vertical size. The critical disturbances of the stream function and temperature (24), (25) are shown in Fig. 2*b*. As can be seen, the inclination of the streamfunction level lines exactly corresponds to the inclination of the chip relative to the direction of gravity.

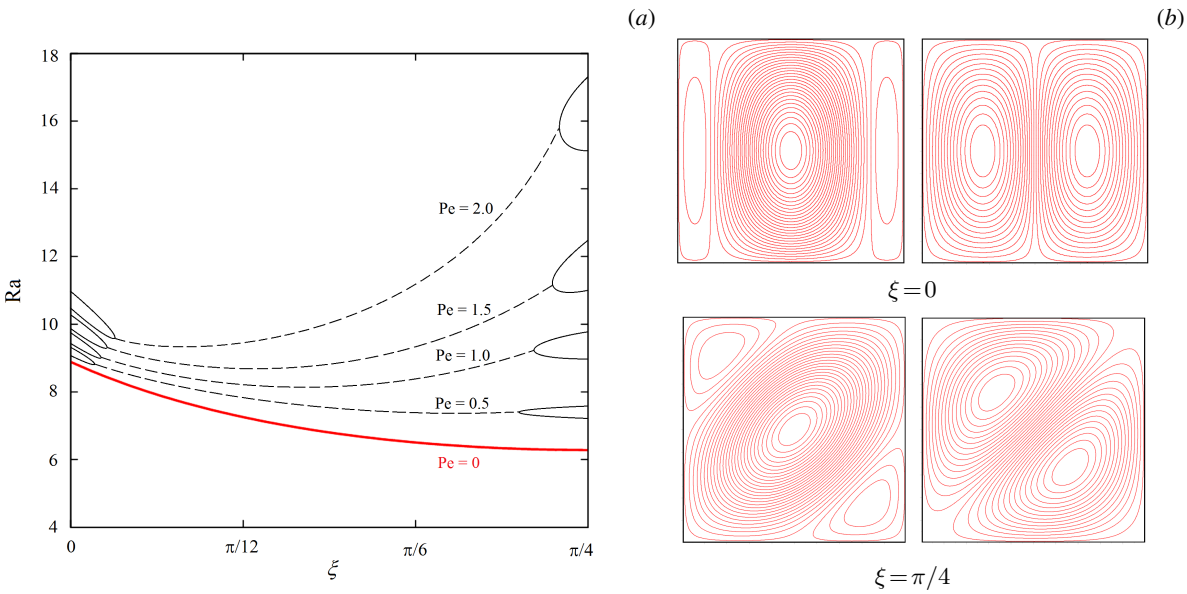


Fig. 2. Neutral curves, above which the basic state is unstable, in the plane of the Rayleigh number Ra and the chip inclination angle ξ for different values of the Péclet number Pe: thin solid and dashed lines correspond to monotonic and oscillatory instability, respectively, while the thick solid line is the doubly degenerate neutral curve for the problem with cosymmetry (19) (*a*); level lines of the critical disturbances of the stream function (*b*) and temperature (*c*), constructed from the analytical solution (24), (25) for two values of the rotation parameter ξ in the absence of pumping ($\mathrm{Pe}=0$)

When fluid is pumped through the chip (porous block) ($\mathrm{Pe}\neq 0$), expressing the solution in terms of elementary functions is apparently impossible. Therefore, to determine the neutral curves, we resort to the Galerkin method. As the basis for approximating ψ and θ, we choose the eigenfunctions of problem (22):

$$\Omega_i(x,y)=\Omega_{(k,m)}(x,y)=\cos(k\pi x)\cos(m\pi y).$$

In [23], the procedure for applying the method is described in detail and the expressions for the expansion coefficients are given. As is well known, in the Galerkin method the accuracy depends on the number of basis functions used in the

approximation. In the present work, the number of functions was increased until the calculation results reached saturation. In most computational experiments, the number of basis functions exceeded 100. Appendix 1 contains a brief description of the solution method.

Let us return to Fig. 2*a*. When pumping appears ($\mathrm{Pe}>0$), cosymmetry is destroyed and the double degeneracy is lifted. It is worth noting that the removal of degeneracy can occur in two ways: at values of the angle ξ for which the chip is close to symmetric configurations (a square at $\xi=0$ and a rhombus at $\xi=\pi/4$), the interacting modes split, and the flow loses stability monotonically (solid lines in the figure). We also note that, in this case, a significant stabilizing effect appears at $\xi=\pi/4$, which is explained by the displacement of disturbances into the upper corner of the rhombus, from which it is more difficult to amplify convection. In a strongly asymmetric domain, the loss of stability occurs in an oscillatory manner (see dashed lines).

4. Branching equation for weakly nonlinear solutions on the slow manifold

Consider the issue of solution branching near the first bifurcation point $\mathrm{Ra}_0(\xi)$, where the basic state (8), (9), under a weak disturbance, is replaced by convective motion both in the cosymmetric and in the symmetric problem. For definiteness, we perturb the flow in a square chip, assuming $\xi \ll 1$ (see Fig. 2*a*). In this case, the complete nonlinear problem (11)–(13) is simplified and reduced to the following:

$$\begin{gathered}\Delta\psi-\mathrm{Ra}\frac{\partial\theta}{\partial x}=-\mathrm{Ra}\xi\frac{\partial\theta}{\partial y},\\ \Delta\theta+\mathrm{Ra}\frac{\partial\psi}{\partial x}=\frac{\partial\theta}{\partial t}+J(\psi,\theta)-\mathrm{Pe}\,\mathrm{Ra}\,y\frac{\partial\psi}{\partial x}+\mathrm{Ra}\xi\frac{\partial\psi}{\partial y}+\mathrm{Pe}\frac{\partial\theta}{\partial y},\\ \psi|_G=0,\quad \theta|_G=0.\end{gathered}\tag{26}$$

To analyze weakly nonlinear solutions, we use the method of multiple time scales [26], which makes it possible to find the governing equations on the slow manifold that always exists in a small neighborhood of the bifurcation point. Following the idea of the method, we seek a solution of problem (26) in the form of expansions in small deviations ε from the basic state:

$$\begin{pmatrix}\mathrm{Ra}\\ \mathrm{Pe}\\ \xi\\ \psi(x,y)\\ \theta(x,y)\\ \dfrac{\partial}{\partial t}\end{pmatrix}=\begin{pmatrix}2\sqrt{2}\pi\\ 0\\ 0\\ 0\\ 0\\ 0\end{pmatrix}+\varepsilon\begin{pmatrix}\mathrm{Ra}_1\\ \mathrm{Pe}_1\\ \xi_1\\ \psi_1(x,y)\\ \theta_1(x,y)\\ \dfrac{\partial}{\partial t_1}\end{pmatrix}+\varepsilon^2\begin{pmatrix}\mathrm{Ra}_2\\ \mathrm{Pe}_2\\ \xi_2\\ \psi_2(x,y)\\ \theta_2(x,y)\\ \dfrac{\partial}{\partial t_2}\end{pmatrix}+\varepsilon^3\begin{pmatrix}\mathrm{Ra}_3\\ \mathrm{Pe}_3\\ \xi_3\\ \psi_3(x,y)\\ \theta_3(x,y)\\ \dfrac{\partial}{\partial t_3}\end{pmatrix}+O(\varepsilon^4).\tag{27}$$

As can be seen from (27), not only the functions but also the problem parameters, as well as the time derivative, are expanded in a series. The latter is a key feature of the method. Since it is not known in advance how time evolves on the slow manifold, it is necessary to determine the hierarchy of times in the course of the analysis in order to find the required scale. For the slow times in (27), we introduce the notation $t_n=\varepsilon^n t$, where the formal small parameter ε characterizes the degree of supercriticality. Substituting (27) into (26) and collecting terms of the same order of smallness n, we arrive at a series of problems, each of which refines its solution from the preceding step. The boundary-value problem for critical disturbances in a square chip heated strictly from below, with the approximation order of the solution $O(\varepsilon)$, takes the form:

$$\Delta\psi_1-2\sqrt{2}\pi\frac{\partial\theta_1}{\partial x}=0,\quad \Delta\theta_1+2\sqrt{2}\pi\frac{\partial\psi_1}{\partial x}=0,\quad \psi_1|_{x=\pm\frac{1}{2},y=\pm\frac{1}{2}}=0,\quad \theta_1|_{x=\pm\frac{1}{2},y=\pm\frac{1}{2}}=0.\tag{28}$$

As shown above (see expressions (23)–(25)), the solution of (28) is given by two pairs of eigenfunctions:

$$\begin{aligned}{\psi_1}^{(1)}(x,y)&=\varphi(x,y)=\cos(\sqrt{2}\pi x)\cos(\pi x)\cos(\pi y),\\ {\theta_1}^{(1)}(x,y)&=\vartheta(x,y)=-\sin(\sqrt{2}\pi x)\cos(\pi x)\cos(\pi y),\end{aligned}\tag{29}$$

and

$$\begin{aligned}{\psi_1}^{(2)}(x,y)&=\vartheta(x,y)=-\sin(\sqrt{2}\pi x)\cos(\pi x)\cos(\pi y),\\ {\theta_1}^{(2)}(x,y)&=-\varphi(x,y)=-\cos(\sqrt{2}\pi x)\cos(\pi x)\cos(\pi y).\end{aligned}\tag{30}$$

Therefore, the correct step is to represent the general solution (28) as a linear combination of (29) and (30) with disturbance amplitudes depending on the slow-time scales:

$$\begin{aligned}\psi_1(x,y)&=\alpha(t_1,t_2,...)\varphi(x,y)+\beta(t_1,t_2,...)\vartheta(x,y),\\ \theta_1(x,y)&=\alpha(t_1,t_2,...)\vartheta(x,y)-\beta(t_1,t_2,...)\varphi(x,y).\end{aligned} \tag{31}$$

Problems with the subsequent orders of smallness of the solution error now take the form of inhomogeneous versions of problem (28):

$$\Delta\psi_n-2\sqrt{2}\pi\frac{\partial\theta_n}{\partial x}=F_n,\quad \Delta\theta_n+2\sqrt{2}\pi\frac{\partial\psi_n}{\partial x}=G_n,\quad \psi_n|_{x=\pm\frac{1}{2},y=\pm\frac{1}{2}}=0,\quad \theta_n|_{x=\pm\frac{1}{2},y=\pm\frac{1}{2}}=0, \tag{32}$$

where the order of smallness is $n>1$, and the functions F_n and G_n are determined from problems of order lower than n. It is clear that these functions must have a special form for problems (32) to be solvable.

We introduce the scalar product of two arbitrary vector functions consisting of two components:

$$[\mathbf{A},\mathbf{B}]=\langle A_1,B_1\rangle+\langle A_2,B_2\rangle. \tag{33}$$

In order to obtain the adjoint problem for (28) with respect to the scalar product (33), we represent (32) in operator form:

$$\hat{\mathbf{L}}U=0,\quad \hat{\mathbf{L}}=\begin{pmatrix}\Delta & -2\sqrt{2}\pi\dfrac{\partial}{\partial x}\\ 2\sqrt{2}\pi\dfrac{\partial}{\partial x} & \Delta\end{pmatrix},\quad \mathbf{U}=(\psi_1,\theta_1). \tag{34}$$

Then the adjoint operator must satisfy the relation:

$$[\mathbf{U}^*,\hat{\mathbf{L}}\mathbf{U}]=[\hat{\mathbf{L}}^*\mathbf{U}^*,\mathbf{U}]. \tag{35}$$

Substituting (34) into (35) and using (28), (33), it is easy to verify that the operator is self-adjoint. Consequently, the inhomogeneous problems (32) have a nontrivial solution if and only if the inhomogeneity vector is orthogonal to the solution of the adjoint problem in the sense of the product (33). Since problem (28) has two linearly independent solutions, there are also two solvability conditions:

$$\langle\varphi,F_n\rangle+\langle\vartheta,G_n\rangle=0,\qquad \langle\vartheta,F_n\rangle-\langle\varphi,G_n\rangle=0. \tag{36}$$

After formulating the solvability conditions (36), we write the inhomogeneous problems of the subsequent orders of smallness explicitly. Thus, at $O(\varepsilon^2)$ we have:

$$\begin{gathered}\Delta\psi_2-2\sqrt{2}\pi\frac{\partial\theta_2}{\partial x}=\mathrm{Ra}_1\frac{\partial\theta_1}{\partial x}-2\sqrt{2}\pi\xi_1\frac{\partial\theta_1}{\partial y},\\ \Delta\theta_2+2\sqrt{2}\pi\frac{\partial\psi_2}{\partial x}=\frac{\partial\theta_1}{\partial t_1}+J(\psi_1,\theta_1)-2\sqrt{2}\pi\mathrm{Pe}_1 y\frac{\partial\psi_1}{\partial x}+2\sqrt{2}\pi\xi_1\frac{\partial\psi_1}{\partial y}-\mathrm{Ra}_1\frac{\partial\psi_1}{\partial x}+\mathrm{Pe}_1\frac{\partial\theta_1}{\partial y},\\ \psi_2|_{x=\pm\frac{1}{2},y=\pm\frac{1}{2}}=0,\quad \theta_2|_{x=\pm\frac{1}{2},y=\pm\frac{1}{2}}=0.\end{gathered} \tag{37}$$

At order $O(\varepsilon^3)$, the right-hand side contains quite a number of terms, which have the following form:

$$\begin{gathered}\Delta\psi_3-2\sqrt{2}\pi\frac{\partial\theta_3}{\partial x}=\mathrm{Ra}_1\frac{\partial\theta_2}{\partial x}+\mathrm{Ra}_2\frac{\partial\theta_1}{\partial x}-2\sqrt{2}\pi\left(\xi_1\frac{\partial\theta_2}{\partial y}+\xi_2\frac{\partial\theta_1}{\partial y}\right)-\mathrm{Ra}_1\xi_1\frac{\partial\theta_1}{\partial y},\\ \Delta\theta_{3,}+2\sqrt{2}\pi\frac{\partial\psi_3}{\partial x}=\frac{\partial\theta_1}{\partial t_2}+\frac{\partial\theta_2}{\partial t_1}+J(\psi_1,\theta_2)+J(\psi_2,\theta_1)-2\sqrt{2}\pi y\left(\mathrm{Pe}_1\frac{\partial\psi_2}{\partial x}+\mathrm{Pe}_2\frac{\partial\psi_1}{\partial x}\right)-\mathrm{Ra}_1\mathrm{Pe}_1 y\frac{\partial\psi_1}{\partial x}+\\ +2\sqrt{2}\pi\left(\xi_1\frac{\partial\psi_2}{\partial y}+\xi_2\frac{\partial\psi_1}{\partial y}\right)-\mathrm{Ra}_1\frac{\partial\psi_2}{\partial x}-\mathrm{Ra}_2\frac{\partial\psi_1}{\partial x}+\mathrm{Ra}_1\xi_1\frac{\partial\psi_1}{\partial y}+\mathrm{Pe}_1\frac{\partial\theta_2}{\partial y}+\mathrm{Pe}_2\frac{\partial\theta_1}{\partial y},\\ \psi_3|_{x=\pm\frac{1}{2},y=\pm\frac{1}{2}}=0,\quad \theta_3|_{x=\pm\frac{1}{2},y=\pm\frac{1}{2}}=0.\end{gathered} \tag{38}$$

The solvability conditions (36) for the second-order problem lead to the following dynamic equations on the slow manifold when time varies on the scale t_1:

$$\begin{aligned}\langle\vartheta,\vartheta\rangle\frac{d\alpha}{dt_1}&=2\alpha\left(\mathrm{Ra}_1\left\langle\vartheta,\frac{\partial\varphi}{\partial x}\right\rangle-2\sqrt{2}\pi\xi_1\left\langle\vartheta,\frac{\partial\varphi}{\partial y}\right\rangle+\sqrt{2}\pi\mathrm{Pe}_1\left\langle y\vartheta,\frac{\partial\varphi}{\partial x}\right\rangle\right)+\beta\mathrm{Pe}_1\left\langle\vartheta,\frac{\partial\varphi}{\partial y}\right\rangle,\\ \langle\varphi,\varphi\rangle\frac{d\beta}{dt_1}&=2\beta\left(\mathrm{Ra}_1\left\langle\vartheta,\frac{\partial\varphi}{\partial x}\right\rangle-2\sqrt{2}\pi\xi_1\left\langle\vartheta,\frac{\partial\varphi}{\partial y}\right\rangle+\sqrt{2}\pi\mathrm{Pe}_1\left\langle y\vartheta,\frac{\partial\varphi}{\partial x}\right\rangle\right)-\alpha\mathrm{Pe}_1\left\langle\vartheta,\frac{\partial\varphi}{\partial y}\right\rangle.\end{aligned}\tag{39}$$

Equations (39) have become linear and therefore cannot fully describe the branching of solutions. To satisfy (39), we set the derivatives with respect to t_1 in the left-hand side equal to zero. Since the eigenfunctions of the problem for a square cavity are known (see (29)), the values of the integrals in equations (39) can be evaluated. It is important that functions (29) in the case of a square chip have different parity with respect to reflection along the x axis (see Fig. 2*b*). Therefore, some of the integrals in (39) vanish, while the remaining ones determine the shift of the convection-onset threshold due to pumping:

$$\mathrm{Ra}_1=\zeta\mathrm{Pe}_1=-\mathrm{Pe}_1\sqrt{2}\pi\left\langle y\vartheta,\frac{\partial\varphi}{\partial x}\right\rangle\Big/\left\langle\vartheta,\frac{\partial\varphi}{\partial x}\right\rangle.$$

We proceed to the problem of order $O(\varepsilon^2)$. For it we obtain:

$$\begin{gathered}\Delta\psi_2-2\sqrt{2}\pi\frac{\partial\theta_2}{\partial x}=\zeta\mathrm{Pe}_1\left(\alpha\frac{\partial\vartheta}{\partial x}-\beta\frac{\partial\varphi}{\partial x}\right)-2\sqrt{2}\pi\xi_1\left(\alpha\frac{\partial\vartheta}{\partial y}-\beta\frac{\partial\varphi}{\partial y}\right),\\ \Delta\theta_2+2\sqrt{2}\pi\frac{\partial\psi_2}{\partial x}=(\alpha^2+\beta^2)J(\varphi,\vartheta)+2\sqrt{2}\pi\xi_1\left(\alpha\frac{\partial\varphi}{\partial y}+\beta\frac{\partial\vartheta}{\partial y}\right)+\\ +\alpha\mathrm{Pe}_1\left(-\zeta\frac{\partial\varphi}{\partial x}-2\sqrt{2}\pi y\frac{\partial\varphi}{\partial x}+\frac{\partial\vartheta}{\partial y}\right)-\beta\mathrm{Pe}_1\left(\zeta\frac{\partial\vartheta}{\partial x}+2\sqrt{2}\pi y\frac{\partial\vartheta}{\partial x}+\frac{\partial\varphi}{\partial y}\right),\\ \psi_2|_{x=\pm\frac{1}{2},y=\pm\frac{1}{2}}=0,\quad\theta_2|_{x=\pm\frac{1}{2},y=\pm\frac{1}{2}}=0.\end{gathered}\tag{40}$$

As can be seen from (40), the solution of the inhomogeneous problem can be sought in the form:

$$\psi_2(x,y)=(\alpha^2+\beta^2)\Phi_1(x,y)+\alpha\xi_1\Omega_1(x,y)+\beta\xi_1\Sigma_1(x,y)+\alpha\mathrm{Pe}_1\Theta_1(x,y)+\beta\mathrm{Pe}_1\Psi_1(x,y),\tag{41}$$

$$\theta_2(x,y)=(\alpha^2+\beta^2)\Phi_2(x,y)+\alpha\xi_1\Omega_2(x,y)+\beta\xi_1\Sigma_2(x,y)+\alpha\mathrm{Pe}_1\Theta_2(x,y)+\beta\mathrm{Pe}_1\Psi_2(x,y),\tag{42}$$

where the unknown functions on the right-hand side must satisfy the corresponding boundary-value problems:

$$\begin{gathered}\Delta\Phi_1-2\sqrt{2}\pi\frac{\partial\Phi_2}{\partial x}=0,\quad\Delta\Phi_2+2\sqrt{2}\pi\frac{\partial\Phi_1}{\partial x}=J(\varphi,\vartheta),\quad\Phi_1|_{x=\pm\frac{1}{2},y=\pm\frac{1}{2}}=0,\quad\Phi_2|_{x=\pm\frac{1}{2},y=\pm\frac{1}{2}}=0;\\ \Delta\Omega_1-2\sqrt{2}\pi\frac{\partial\Omega_2}{\partial x}=-2\sqrt{2}\pi\frac{\partial\vartheta}{\partial y},\quad\Delta\Omega_2+2\sqrt{2}\pi\frac{\partial\Omega_1}{\partial x}=2\sqrt{2}\pi\frac{\partial\varphi}{\partial y},\quad\Omega_1|_{x=\pm\frac{1}{2},y=\pm\frac{1}{2}}=0,\quad\Omega_2|_{x=\pm\frac{1}{2},y=\pm\frac{1}{2}}=0;\\ \Delta\Sigma_1-2\sqrt{2}\pi\frac{\partial\Sigma_2}{\partial x}=2\sqrt{2}\pi\frac{\partial\varphi}{\partial y},\ \Delta\Sigma_2+2\sqrt{2}\pi\frac{\partial\Sigma_1}{\partial x}=2\sqrt{2}\pi\frac{\partial\vartheta}{\partial y},\ \Sigma_1|_{x=\pm\frac{1}{2},y=\pm\frac{1}{2}}=0,\ \Sigma_2|_{x=\pm\frac{1}{2},y=\pm\frac{1}{2}}=0;\\ \Delta\Theta_1-2\sqrt{2}\pi\frac{\partial\Theta_2}{\partial x}=0,\quad\Delta\Theta_2+2\sqrt{2}\pi\frac{\partial\Theta_1}{\partial x}=\frac{\partial\vartheta}{\partial y}-2\sqrt{2}\pi y\frac{\partial\varphi}{\partial x},\quad\Theta_1|_{x=\pm\frac{1}{2},y=\pm\frac{1}{2}}=0,\quad\Theta_2|_{x=\pm\frac{1}{2},y=\pm\frac{1}{2}}=0;\\ \Delta\Psi_1-2\sqrt{2}\pi\frac{\partial\Psi_2}{\partial x}=0,\quad\Delta\Psi_2+2\sqrt{2}\pi\frac{\partial\Psi_1}{\partial x}=-\frac{\partial\varphi}{\partial y}-2\sqrt{2}\pi y\frac{\partial\vartheta}{\partial x},\quad\Psi_1|_{x=\pm\frac{1}{2},y=\pm\frac{1}{2}}=0,\quad\Psi_2|_{x=\pm\frac{1}{2},y=\pm\frac{1}{2}}=0.\end{gathered}\tag{43}$$

We proceed to the problem of order $O(\varepsilon^3)$, substitute the solutions (41), (42) into (38), and impose the solvability conditions (36). Some of the terms vanish because of the parity properties of the eigenfunctions (29); the remaining integrals are computed using the Maple computer algebra system. Here we give only the final result — the form of the normal form governing the evolution on the time scale of order t_2:

$$\frac{d\alpha}{d\tau}=\alpha(R-\alpha^2-\beta^2)+P\alpha\beta+P\xi\beta,\tag{44}$$

$$L\frac{d\beta}{d\tau}=\beta(R+DP^2-\alpha^2-\beta^2)+P(B\alpha^2+M\beta^2)-P\xi\alpha,\tag{45}$$

where

$$\tau \equiv \frac{t_2}{\langle \vartheta,\vartheta\rangle}, \quad L \equiv \frac{\langle \varphi,\varphi\rangle}{\langle \vartheta,\vartheta\rangle}, \quad R \equiv 2\mathrm{Ra}_2\left\langle \vartheta, \frac{\partial \varphi}{\partial x}\right\rangle + \mathrm{Pe}_1^2\left(\left\langle \zeta y\vartheta + (y+\zeta)\Psi_1, \frac{\partial \varphi}{\partial x}\right\rangle + \zeta\left\langle \Psi_2, \frac{\partial \vartheta}{\partial x}\right\rangle + \left\langle (\Theta_2-\Psi_1), \frac{\partial \vartheta}{\partial y}\right\rangle\right),$$

$$B \equiv \frac{\left\langle \Phi_1, (1+2\sqrt{2}\pi y)\frac{\partial \varphi}{\partial x}\right\rangle - \langle \Theta_1, J(\varphi,\vartheta)\rangle - \left\langle \Phi_2, \zeta\frac{\partial \vartheta}{\partial x} + \frac{\partial \varphi}{\partial y}\right\rangle}{\langle (\Psi_2-\Theta_1), J(\varphi,\vartheta)\rangle}, \quad D \equiv \frac{\left\langle (\Theta_2-\Psi_1), \frac{\partial \vartheta}{\partial x}\right\rangle - \left\langle \Psi_2, \frac{\partial \varphi}{\partial y}\right\rangle}{\langle (\Psi_2-\Theta_1), J(\varphi,\vartheta)\rangle^2}, \tag{46}$$

$$M \equiv \frac{\left\langle \Phi_1, (1+2\sqrt{2}\pi y)\frac{\partial \varphi}{\partial x}\right\rangle + \langle \Psi_2, J(\varphi,\vartheta)\rangle - \left\langle \Phi_2, \zeta\frac{\partial \vartheta}{\partial x} + \frac{\partial \varphi}{\partial y}\right\rangle}{\langle (\Psi_2-\Theta_1), J(\varphi,\vartheta)\rangle},$$

$$P \equiv \mathrm{Pe}_1\langle (\Psi_2-\Theta_1), J(\varphi,\vartheta)\rangle, \quad \xi \equiv \xi_1 \frac{2\sqrt{2}\pi\left(\left\langle \Psi_1, \frac{\partial \vartheta}{\partial y}\right\rangle + \left\langle \Psi_2, \frac{\partial \varphi}{\partial y}\right\rangle - \left\langle y\Sigma_1, \frac{\partial \vartheta}{\partial x}\right\rangle\right) + \left\langle \Sigma_2, \frac{\partial \vartheta}{\partial y}\right\rangle}{\langle (\Psi_2-\Theta_1), J(\varphi,\vartheta)\rangle}.$$

We note that in equations (44), (45) and in the results presented below, the symmetry imperfection parameter is represented by its leading expansion term ξ_1 (46) without changing the notation. Remarks on the methods for solving the boundary-value problems (43) and computing the integrals (46) are given in Appendix 2.

Let us consider two limiting cases for system (44), (45). For fluid pumping through a chip symmetric with respect to horizontal reflection ($\xi = 0$), we obtain the equations:

$$\frac{d\alpha}{d\tau} = \alpha(R-\alpha^2-\beta^2) + P\alpha\beta,$$

$$L\frac{d\beta}{d\tau} = \beta(R+DP^2-\alpha^2-\beta^2) + P(B\alpha^2+M\beta^2),$$

which are analogous to those considered earlier in [23]. The reflection symmetry of the physical problem manifests itself in the invariance of both the equations and the phase space under the transformation $\alpha \to -\alpha$.

In a strongly asymmetric chip, $\xi \gg 0$, and at low fluid pumping velocities, the equations on the plane take the form:

$$\frac{d\alpha}{d\tau} = \alpha(R-\alpha^2-\beta^2) + P\xi\beta,$$

$$L\frac{d\beta}{d\tau} = \beta(R-\alpha^2-\beta^2) - P\xi\alpha,$$

and, in essence, coincide with the normal form of the Andronov–Hopf bifurcation for the branching of a limit cycle. Thus, the model equations (44), (45) describe the transition between these two limiting cases.

5. Bifurcation analysis

Although the dynamical system (44), (45) has only second-order accuracy, the study of its bifurcation structure requires the use of a computer. It is convenient to use a suitable symbolic computation system, for example Maple. In the general case, when the parameters ξ and P are nonzero, the system has neither symmetries nor cosymmetries. Numerous equilibrium states move arbitrarily over the phase plane and collide with one another. In this case, bifurcation diagrams are best constructed by the continuation method, which involves moving along a parameter with a small step. To compute the new positions of fixed points, their coordinates from the previous step should be used as initial values for the search. The change in stability of the trivial equilibrium can now be studied analytically.

Figure 3 represents a stability map of the convective flow constructed for the dynamical system described by equations (44), (45), with the following values of the integrals and parameters (46):

$$L \approx 1.6, \quad M \approx 2.4, \quad B \approx 1.4, \quad D \approx 1.8, \quad P = 1. \tag{47}$$

Variation of the Péclet number does not qualitatively change the branching scenario and only leads to scaling of the stability map; therefore, it was fixed in (47). To better understand the branching of solutions with variation of the inclination angle, which plays the role of the imperfection parameter of the chip reflection symmetry, Fig. 4 shows

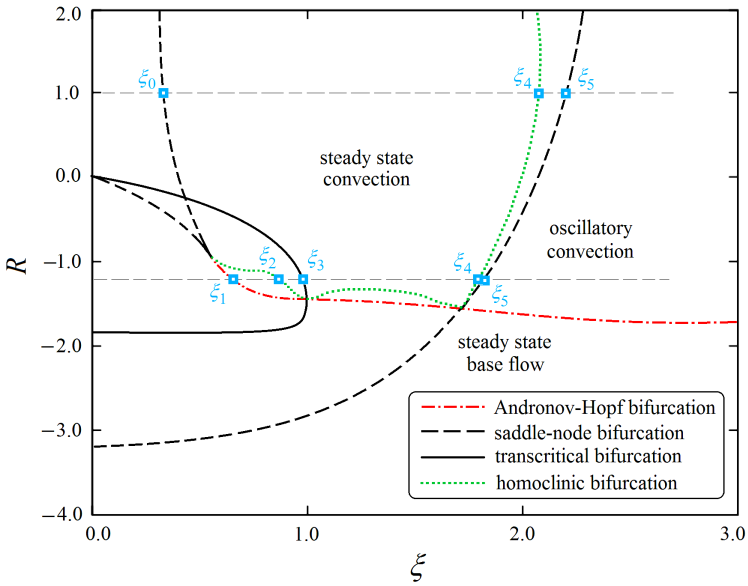


Fig. 3. Stability map in the plane of the parameters "symmetry imperfection ξ–supercriticality R" at a fixed value of the pumping parameter P=1 and for different types of bifurcations; dashed horizontal lines indicate the positions of two characteristic sections of the stability map

bifurcation diagrams in two characteristic horizontal sections of the stability map. As can be seen from the figure, the bifurcation structure of the system obtained near the first bifurcation point appears nonstandard and complicated. One can observe multiplicity of stationary solutions and their branching (thick solid and dashed lines), soft branching of limit cycles through the Andronov–Hopf bifurcation (thick solid lines with arrows), as well as homoclinic bifurcations (see dotted lines, Fig. 3). The reason for this behavior lies in the property of cosymmetry possessed by the system in the absence of fluid pumping through the porous block ($\mathrm{Pe}=0$). In this case, in the supercritical region, a cycle of equilibria branches off from the trivial equilibrium:

$$\alpha^2+\beta^2=R. \tag{48}$$

Under fluid pumping, the cosymmetry of the system is destroyed. We first consider the sequence of solution branching in a chip that is perfectly symmetric with respect to horizontal reflection ($\xi=0$). Figure 4 shows that the phase portrait of the system includes four nontrivial equilibria, each corresponding to a particular type of steady convection:

$$O_{1,2}: \quad \alpha_{1,2}=0, \quad \beta_{1,2}=MP/2\pm\sqrt{(M^2+4D)P^2+4R}; \tag{49}$$

$$O_{3,4}: \quad \alpha_{3,4}=\pm\sqrt{R-\beta_{3,4}^2+P(M-B)\beta_{3,4}}, \quad \beta_{3,4}=-\frac{BR}{P(D+B(M-B))}. \tag{50}$$

As follows from formula (49), the pair of equilibria $O_{1,2}$ appears in the subcritical region of the parameter R owing to a saddle-node bifurcation at $R^*=-P^2(M^2+4D)/4$.

The vertical flow stimulates the emergence of solutions of a certain symmetry, in this case two-vortex convection (30), governed by the amplitude β. Of the two points, only one solution is stable, namely the solution for which the direction of the central jet coincides with the direction of the basic flow. On the stability map, this branch begins in the lower left corner (dashed line, Fig. 3). With increasing supercriticality, one of the solutions (49) crosses the trivial equilibrium at $R^{**}=-DP^2$ and exchanges stability with it (thick solid line in Fig. 3).

At $R=0$, a pair of solutions (50) corresponding to motion of another parity branches off from the trivial equilibrium through a pitchfork bifurcation. The solutions (29), governed by the amplitude α, represent three-vortex flows. Vertical pumping suppresses them, and therefore they are unstable. The phase portrait of the system for a square chip is presented in Fig. 4*a* on the left for the case $R=1$, when the solutions at all four fixed points have already branched off. As can be seen from the figure, the pair of points (49) attracts all trajectories, which partition the phase space.

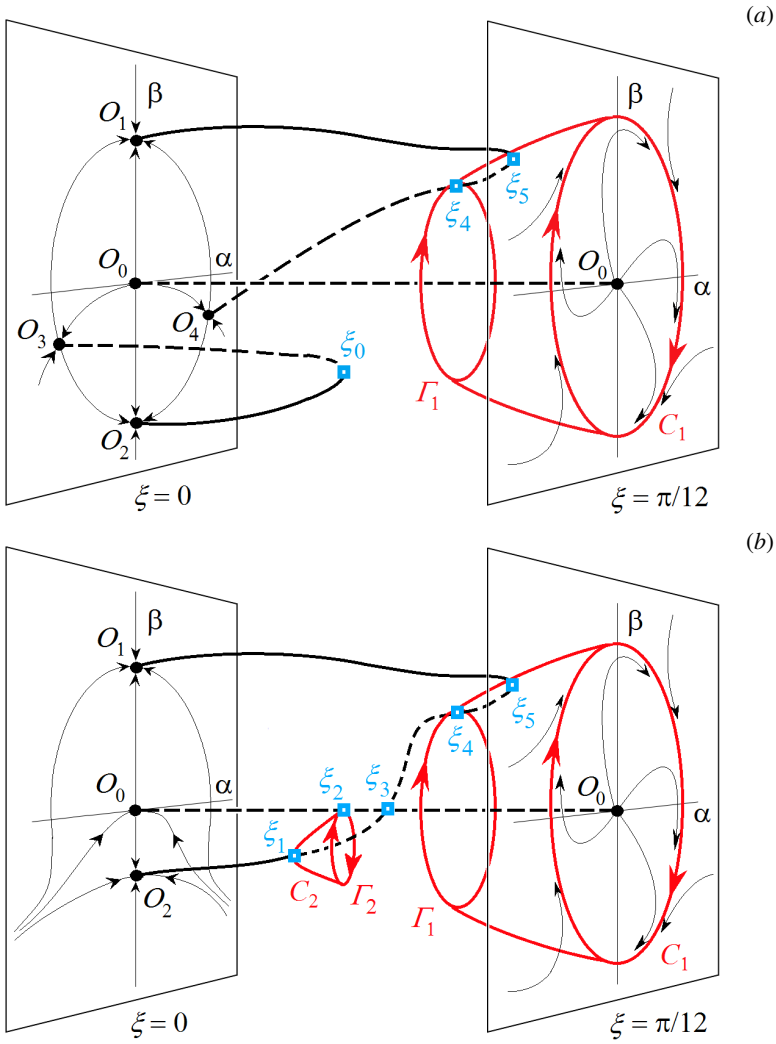


Fig. 4. Bifurcation diagrams in characteristic sections of the stability map in Fig. 3 for different chip inclination angles ξ and different values of the supercriticality parameter R: 1.0 (*a*), −1.2 (*b*)

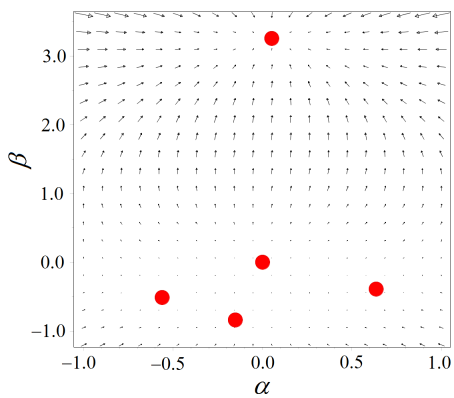


Fig. 5. Vector field and attracting fixed points of the dynamical system (44), (45) at $R = 1.0$, $P = 1.0$, $\xi = 0.1$, computed using the Maple package; the Maple program for analyzing the bifurcation structure of the dynamical system is available at https://journal.permsc.ru/index.php/ccm/ru/article/view/CCMv19n1a4

Let us now trace how the branching of solutions occurs under gradual symmetry broken with the chip. As can be seen from the diagram (Fig. 4*a*), when the cavity is inclined, the nontrivial solutions (49) and (50) begin to approach one another pairwise. This moment is also shown in the phase portrait in Fig. 5. At $\xi = \xi_0$, the pair of equilibria O_2 and O_3 merges and disappears due to a saddle-node bifurcation. The second pair, O_1 and O_4, shifts into the first quadrant, which describes convective motions with a preferred sense of rotation. At $\xi = \xi_4$, a homoclinic trajectory Γ_1 is formed at the saddle equilibrium O_4, and when it breaks, a limit cycle C_1 is generated in a hard manner. With further motion into the asymmetry region, the equilibria O_1 and O_4 merge and disappear at $\xi = \xi_5$. Only the limit cycle C_1 remains in the phase space of the system, attracting all trajectories.

In another section of the stability map ($R = -1.2$), the bifurcation diagram for a symmetric cuvette ($\xi = 0$) contains only two nontrivial equilibria, which begin to shift into the first quadrant as the symmetry imperfection parameter is varied. The type of solution changes in this process. The equilibrium point O_2 becomes a focus instead of a node. At $\xi = \xi_1$, an Andronov–Hopf bifurcation occurs and a stable limit cycle C_2 is born softly. This exotic solution exists only in a narrow region of the stability map between the dash-dotted and dotted lines (see Fig. 3). Very quickly, the cycle encounters the saddle trivial equilibrium and disappears through a reverse homoclinic bifurcation at $\xi = \xi_2$. Exchanging stability with the zero equilibrium at $\xi = \xi_3$, the point O_2 enters the first quadrant, where the scenario described above for the diagram in Fig. 4*a* is then repeated.

6. Discussion

In recent years, the formulation of the problem of the stability of a nonisothermal fluid seeping through a porous medium has again become relevant due to the rapid development of microfluidic devices and the emergence of technologies for growing cellular tissues. As a rule, a perfusion bioreactor includes a scaffold intended to support cell growth, which, in essence, appears as a porous chip of a certain structure through which a nutrient solution for the cells is pumped. Cells are seeded into the porous matrix, where they attach to the pore walls; then, under the action of the flow, they divide and gradually fill the pore space. To maintain favorable conditions for cell proliferation, the system is heated in a certain way. In the application of such devices, emphasis is placed on finding methods to control the flows of substances within scaffolds, since cells are sensitive to changes in the shear-stress field and to growth factors. The class of porous chips whose mathematical formulation admits the presence of cosymmetry/symmetry properties is of interest because slight variations in their geometric parameters lead to abrupt changes in the flow characteristics. In the present work, it is shown that small changes (within a few degrees) in the orientation of a square chip relative to the direction of fluid pumping cause a complex restructuring of the flow in them — from steady to oscillatory. Thus, by varying the symmetry imperfection parameter of the problem, one can switch the operating regimes of a perfusion bioreactor.

We note that, in the original mathematical formulation of the problem (2)–(6), the role of the chip was played by an infinitely extended cylinder. This was required in order for translational symmetry in the direction of the cylinder axis to appear in the problem. From a mathematical point of view, this made it possible to formally consider only the class of two-dimensional solutions that do not depend on the axial coordinate. This would seem to contradict the pumping region in the form of a finite chip used in the present work (see Fig. 1); however, from a physical point of view, two-dimensional flows can pose a threat precisely in short cylinders. For example, in [27] it was shown that, in a cylinder of square cross section, three-dimensional disturbances become more dangerous if the cylinder length begins to exceed a value equal to 0.23 of the side of the square. If the cylinder is shorter, then three-dimensional disturbances in it are stabilized, and the stability problem coincides with the problem presented in the present work.

7. Conclusion

Convective motions in a porous cylinder of square cross section heated from below and slightly inclined with respect to gravity in the cross-sectional plane (chip) have been investigated. The porous medium is embedded in a solid massif of high thermal conductivity, and uniform pumping of fluid through the system is carried out in the vertical direction. A stability map has been constructed, and the branching structure of weakly nonlinear solutions in a small neighborhood of the first bifurcation point has been studied.

Appendix 1

We consider the problem of convective motions (11)–(13) in a square cavity $0 \leqslant x \leqslant 1$, $0 \leqslant y \leqslant 1$ with a square membrane fixed along its edges. Taking into account the spatial symmetry and boundary conditions, we choose the

eigenfunctions of mechanical vibrations of the membrane as the basis for approximating the unknown variables of the problem:

$$f_i(x,y)=2\sin(k\pi x)\sin(m\pi y)\quad (i,k,m=1,2,3...), \tag{51}$$

normalized as follows:

$$\langle f_i,f_j\rangle=\delta_{ij},\quad \langle f_i,\Delta f_j\rangle=-\omega_i\delta_{ij},\quad \omega_i=-(k^2+m^2)\pi^2.$$

We represent disturbances of the stream function and temperature in the form of expansions:

$$\psi(t,x,y)=\sum_{n=1}^{N}a_n(t)f_n(x,y),\quad \theta(t,x,y)=\sum_{n=1}^{N}b_n(t)f_n(x,y), \tag{52}$$

where a_n, b_n — are the unknown coefficients, which in general depend on time. According to the Galerkin method, they are determined from the requirement of orthogonality to the system of trial functions (51) of the differential operators L_ψ and L_θ, defined, respectively, by equations (11) and (12):

$$\langle f_i(x,y),L_\psi(x,y)\rangle=0,\quad \langle f_i(x,y),L_\theta(x,y)\rangle=0. \tag{53}$$

Substituting the expansions (52) into equations (11), (12) and integrating expressions (53), we arrive at a system of N autonomous first-order ordinary differential equations. In the general case, the constructed system is nonlinear and can be used to study the nonlinear dynamics of the original problem (11)–(13) at high supercriticalities. In the present work, a more modest task was posed: to investigate the stability of the basic flow (8), (9) in the linear approximation. Neglecting nonlinear terms in (53) and assuming the coefficients a_n, b_n to be independent of time, we obtain the following system of homogeneous linear equations:

$$-\omega_i^2 b_i+\frac{\mathrm{Ra}^2\mathrm{Pe}}{2\mathrm{sh}\left(\frac{1}{2}\mathrm{Pe}\right)}\left(\cos(\xi)\sin(\xi)\sum_{n,l=1}^{N}\frac{L_{in}D_{nl}+N_{in}B_{nl}}{\omega_n^2}b_l-\cos^2(\xi)\sum_{n,l=1}^{N}\frac{L_{in}B_{nl}}{\omega_n^2}b_l-\sin^2(\xi)\sum_{n,l=1}^{N}\frac{N_{in}D_{nl}}{\omega_n^2}b_l\right)-$$

$$-\mathrm{Pe}\left(\sin(\xi)\sum_{n=1}^{N}B_{in}b_n+\cos(\xi)\sum_{n=1}^{N}D_{in}b_n\right)=0. \tag{54}$$

Here the nonzero elements of the matrices have the form:

$$B_{ij}=B_{(k,m),(l,n)}=\frac{4kl}{k^2-l^2},\quad \text{if } m=n,\ k+l=odd,$$

$$D_{ij}=D_{(k,m),(l,n)}=\frac{4mn}{m^2-n^2},\quad \text{if } k=l,\ m+n=odd, \tag{55}$$

$$L_{ij}=L_{(k,m),(l,n)}=\frac{16\pi^2 nklm\mathrm{Pe}\cos(\xi)(\cos((m+n)\pi)e^{\mathrm{Pe}\cos(\xi)}-1)}{(k^2-l^2)(\mathrm{Pe}^2\cos^2(\xi)+\pi^2(m-n)^2)(\mathrm{Pe}^2\cos^2(\xi)+\pi^2(m+n)^2)},\quad \text{if } k+l=odd,$$

$$N_{ij}=N_{(k,m),(l,n)}=\frac{16\pi^2 nklm\mathrm{Pe}\sin(\xi)(\cos((k+l)\pi)e^{\mathrm{Pe}\sin(\xi)}-1)}{(m^2-n^2)(\mathrm{Pe}^2\sin^2(\xi)+\pi^2(k-l)^2)(\mathrm{Pe}^2\sin^2(\xi)+\pi^2(k+l)^2)},\quad \text{if } m+n=odd.$$

The procedure for investigating the linear stability of the basic state involves computing the eigenvalues of the matrix defined by expressions (54), (55) and identifying the moment when, as the control parameters of the problem are varied, the increment first crosses the imaginary axis. Since the matrix coefficients (55) are obtained in general form, refinement of the critical value can be organized by automatically adding new basis functions until the value found reaches saturation within the prescribed accuracy of the solution.

Appendix 2

The boundary-value problems (43) and the integral relations (46) are implemented using the Maple symbolic computation system. To simplify the procedure, it is useful to employ integral transformations. The first boundary-value

problem in the list (46) is solved relatively simply, since a particular solution satisfying the boundary conditions has the following form:

$$\Phi_1(x,y)=\frac{1}{16}\sin(2\pi x)\sin(2\pi y),\quad \Phi_2(x,y)=\frac{\sqrt{2}}{16}(\sin(2\pi y)+\cos(2\pi x)\sin(2\pi y)). \tag{56}$$

The solution of the remaining boundary-value problems is rather cumbersome. It can be noted, however, that owing to the particular parity of the integrals (46), not all boundary-value problems need to be solved. For example, the functions Σ_1 and Σ_2 are required only in the integrals entering the rescaled imperfection parameter. The functions Ω_1 and Ω_2 do not enter expressions (46) at all. At the same time, the functions Θ_i, Ψ_i are used extensively.

As an example, consider the coefficient M. To determine it, one must compute the value of the integral $\langle\Theta_1,J(\varphi,\vartheta)\rangle$. We show that this can be done without solving the boundary-value problem for Θ_1 and Θ_2 from the list (43). We multiply the equation for Φ_2 by Θ_1 and integrate over the square domain. At the same time, we multiply the equation for Θ_2 by Φ_1 and also integrate over the domain. Then, respectively, we obtain:

$$\langle\Theta_1,\Delta\Phi_2\rangle+2\sqrt{2}\pi\left\langle\Theta_1,\frac{\partial\Phi_1}{\partial x}\right\rangle=\langle\Theta_1,J(\varphi,\vartheta)\rangle, \tag{57}$$

$$\langle\Phi_1,\Delta\Theta_2\rangle+2\sqrt{2}\pi\left\langle\Phi_1,\frac{\partial\Theta_1}{\partial x}\right\rangle=\left\langle\Phi_1,\frac{\partial\vartheta}{\partial y}\right\rangle-2\sqrt{2}\pi\left\langle\Phi_1,y\frac{\partial\varphi}{\partial x}\right\rangle. \tag{58}$$

The required integral has appeared on the right-hand side of (57). The integrals on the right-hand side of (58) are readily computed, since all integrand functions are already known. Performing integration by parts and taking into account the boundary conditions in (43), we carry out the following transformations of the integrals on the left-hand side of (58):

$$\langle\Phi_1,\Delta\Theta_2\rangle=\langle\Theta_2,\Delta\Phi_1\rangle=2\sqrt{2}\pi\left\langle\Theta_2,\frac{\partial\Phi_2}{\partial x}\right\rangle=-2\sqrt{2}\pi\left\langle\Phi_2,\frac{\partial\Theta_2}{\partial x}\right\rangle=-\langle\Phi_2,\Delta\Theta_1\rangle=-\langle\Theta_1,\Delta\Phi_2\rangle; \tag{59}$$

$$2\sqrt{2}\pi\left\langle\Phi_1,\frac{\partial\Theta_1}{\partial x}\right\rangle=-2\sqrt{2}\pi\left\langle\Theta_1,\frac{\partial\Phi_1}{\partial x}\right\rangle.$$

In the transformations in (59), the equations for Φ_1 and Θ_1 were used. Comparing expressions (57) and (58), we see that their right-hand sides are equal in magnitude and opposite in sign. Finally, we obtain:

$$\langle\Theta_1,J(\varphi,\vartheta)\rangle=2\sqrt{2}\pi\left\langle\Phi_1,y\frac{\partial\varphi}{\partial x}\right\rangle-\left\langle\Phi_1,\frac{\partial\vartheta}{\partial y}\right\rangle.$$

Thus, the required integral is expressed through an integral of already known functions. All integrals in (46) can be computed in a similar manner.

The research was supported by the Russian Science Foundation (project No. 25-11-00338).

References

1. *Nield D.A.*, *Bejan A.* Convection in Porous Media. Springer International Publishing, 2017. 988 p. DOI: 10.1007/978-3-319-49562-0
2. *Siraev R.R.* Fluid transport in Forchheimer porous medium with spatially varying porosity and permeability. Computational Continuum Mechanics. 2019. Vol. 12, no. 3. P. 281–292. DOI: 10.7242/1999-6691/2019.12.3.24
3. *Maryshev B.S.*, *Lyubimova T.P.*, *Lyubimov D.V.* Stability of homogeneous seepage of a liquid mixture through a closed region of the saturated porous medium in the presence of the solute immobilization. International Journal of Heat and Mass Transfer. 2016. Vol. 102. P. 113–121. DOI: 10.1016/j.ijheatmasstransfer.2016.06.016
4. *Kolchanova E.A.*, *Kolchanov N.V.* Convective solute transport in a sloping two-layered active porous medium with a pore clogging effect. International Communications in Heat and Mass Transfer. 2025. Vol. 161. P. 108526. DOI: 10.1016/j.icheatmasstransfer.2024.108526
5. *De Wit A.* Chemo-Hydrodynamic Patterns and Instabilities. Annual Review of Fluid Mechanics. 2020. Vol. 52, no. 1. P. 531–555. DOI: 10.1146/annurev-fluid-010719-060349

6. *Varma M.V.*, *Kandasubramanian B.*, *Ibrahim S.M.* 3D printed scaffolds for biomedical applications. Materials Chemistry and Physics. 2020. Vol. 255. P. 123642. DOI: 10.1016/j.matchemphys.2020.123642

7. *Zhianmanesh M.*, *Varmazyar M.*, *Montazerian H.* Fluid Permeability of Graded Porosity Scaffolds Architectured with Minimal Surfaces. ACS Biomaterials Science &; Engineering. 2019. Vol. 5, no. 3. P. 1228–1237. DOI: 10.1021/acsbiomaterials.8b01400

8. *Krasnyakov I.*, *Bratsun D.* Cell-Based Modeling of Tissue Developing in the Scaffold Pores of Varying Cross-Sections. Biomimetics. 2023. Vol. 8. P. 562. DOI: 10.3390/biomimetics8080562

9. *Bratsun D.*, *Elenskaya N.*, *Siraev R.*, *Tashkinov M.* Numerical Analysis of Permeability of Functionally Graded Scaffolds. Fluid Dynamics & Materials Processing. 2024. Vol. 20, no. 7. P. 1463–1479. DOI: 10.32604/fdmp.2024.047928

10. *Bratsun D.*, *Kostarev K.* Phase Transition in a Dense Swarm of Self-Propelled Bots. Fluid Dynamics & Materials Processing. 2024. Vol. 20, no. 8. P. 1785–1798. DOI: 10.32604/fdmp.2024.048206

11. *Lapwood E.R.* Convection of a fluid in a porous medium. Mathematical Proceedings of the Cambridge Philosophical Society. 1948. Vol. 44, no. 4. P. 508–521. DOI: 10.1017/S030500410002452X

12. *Riley D.S.*, *Winters K.H.* Modal exchange mechanisms in Lapwood convection. Journal of Fluid Mechanics. 1989. Vol. 204. P. 325–358. DOI: 10.1017/S0022112089001771

13. *Gershuni G.Z.*, *Zhuhovitsky E.M.* Convective Stability of Incompressible Fluids. Jerusalem: Keter Publishing House, 1976. 330 p.

14. *Lyubimov D.V.* Convective motions in a porous medium heated from below. Journal of Applied Mechanics and Technical Physics. 1975. Vol. 16, no. 2. P. 257–261. DOI: 10.1007/BF00858924

15. *Glukhov A.F.*, *Lyubimov D.V.*, *Putin G.F.* Konvektivnyye dvizheniya v poristoy srede vblizi poroga neustoychivosti ravnovesiya. Doklady Akademii nauk SSSR. 1978. Vol. 238, no. 3. P. 549–551.

16. *Yudovich V.I.* Cosymmetry, degeneration of solutions of operator equations, and onset of a filtration convection. Mathematical Notes of the Academy of Sciences of the USSR. 1991. Vol. 49. P. 540–545. DOI: 10.1007/BF01142654

17. *Yudovich V.I.* Secondary cycle of equilibria in a system with cosymmetry, its creation by bifurcation and impossibility of symmetric treatment of it. Chaos: An Interdisciplinary Journal of Nonlinear Science. 1995. Vol. 5, no. 2. P. 402–411. DOI: 10.1063/1.166110

18. *Govorukhin V.N.*, *Yudovich V.I.* Bifurcations and selection of equilibria in a simple cosymmetric model of filtrational convection. Chaos: An Interdisciplinary Journal of Nonlinear Science. 1999. Vol. 9, no. 2. P. 403–412. DOI: 10.1063/1.166417

19. *Yudovich V.I.* Bifurcations under perturbations violating cosymmetry. Doklady Physics. 2004. Vol. 49. P. 522–526. DOI: 10.1134/1.1810578

20. *Tsybulin V.G.*, *Karasözen B.*, *Ergenç T.* Selection of steady states in planar Darcy convection. Physics Letters A. 2006. Vol. 356, no. 3. P. 189–194. DOI: 10.1016/j.physleta.2006.03.043

21. *Karasözen B.*, *Trofimova A.V.*, *Tsybulin V.G.* Natural convection in porous annular domains: Mimetic scheme and family of steady states. Journal of Computational Physics. 2012. Vol. 231, no. 7. P. 2995–3005. DOI: 10.1016/j.jcp.2012.01.004

22. *Kurakin L.G.*, *Kurdoglyan A.V.* Semi-Invariant Form of Equilibrium Stability Criteria for Systems with One Cosymmetry. Russian Journal of Nonlinear Dynamics. 2019. Vol. 15, no. 4. P. 525–531. DOI: 10.20537/nd190411

23. *Bratsun D.A.*, *Lyubimov D.V.*, *Roux B.* Co-symmetry breakdown in problems of thermal convection in porous medium. Physica D: Nonlinear Phenomena. 1995. Vol. 82. P. 398–417. DOI: 10.1016/0167-2789(95)00045-6

24. *Nilsen T.*, *Storesletten L.* An Analytical Study on Natural Convection in Isotropic and Anisotropic Porous Channels. Journal of Heat Transfer. 1990. Vol. 112. P. 396–401. DOI: 10.1115/1.2910390

25. *Storesletten L.*, *Tveitereid M.* Natural convection in a horizontal porous cylinder. International Journal of Heat and Mass Transfer. 1991. Vol. 34. P. 1959–1968. DOI: 10.1016/0017-9310(91)90207-U

26. *Nayfeh A.H.* Introduction in perturbation techniques. New York: Wiley-VCH, 1981. 533 p.

Author's Details:

Bratsun Dmitriy Anatolyevich, Dr. Sci. (Phys.-Math.), Assoc. Prof., Head of Department, Perm National Research Polytechnic University (PNRPU), 614990, Perm, Komsomolsky Ave., 29; e-mail: DABracun@pstu.ru; ORCID: 0000-0002-3229-2330